This is the authors' version of the article published in Macromolecules. Changes were made to this version by the publisher prior to publication. The final version is available at 10.1021/acs.macromol.0c01231

Advancing the synthesis of isocyanate-free poly(oxazolidones)s: scope and limitations

Thomas Habets,[a] Fabiana Siragusa,[a] Bruno Grignard,[a] Christophe Detrembleur [a]*

[a] Center for Education and Research on Macromolecules (CERM), CESAM Research Unit, University of Liege, Sart-Tilman B6a, 4000 Liege, Belgium

* **E-mail**: Christophe.Detrembleur@ULiege.be

Abstract

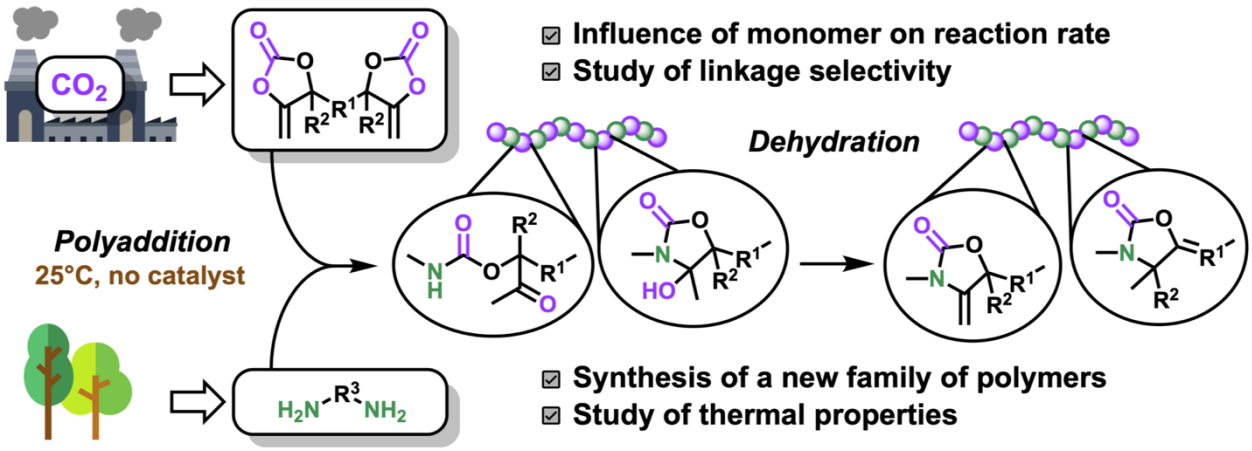

Poly(oxazolidone) is an emerging class of polyurethanes that is easily accessible by an isocyanate-free pathway via the step-growth copolymerization of CO_2-based monomers (bis(α-alkylidene cyclic carbonate)s) with primary diamines at room temperature. Here we explore the scope and limitation of this process by investigating the influence of the diamine and the reaction conditions on the structure and macromolecular parameters of the polymer. Less hindered diamines (aliphatic and benzylic) provide selectively

poly(hydroxyoxazolidone)s, whereas the bulkier ones (cycloaliphatic) furnish polymer chains bearing two types of linkages, oxo-urethane and hydroxyoxazolidone ones. The increase of the reaction temperature or the addition of DBU as catalyst enables to accelerate the polymerizations. The quantitative polymer dehydration is also achieved by refluxing in acetic acid, providing a new class of unsaturated poly(oxazolidone)s constituted of α-alkylidene oxazolidone linkages (for hindered polymers), or a mixture of α- and β-alkylidene oxazolidones linkages (for the less hindered ones). These unsaturated poly(oxazolidone)s present a high glass transition temperature (90 °C$\leq T_g \leq$ 130 °C) and a remarkable thermal stability (T_d > 360 °C), rendering these polymers attractive for applications requiring high temperatures. This work is therefore opening an avenue to novel functional isocyanate-free PUs, with the pendant hydroxyl or olefin groups that are expected to be easily derivatized.

Introduction

Polyurethanes (PUs) account for 8 % of the total plastic demand, which corresponds to a production of 16 millions of tons for the world market[1,2]. The industrial production of PUs is based on the polyaddition of diisocyanates with diols,[3,4] with the advantage that many different types of diols (petro- and/or bio-sourced) are accessible at low cost, giving access to cost-effective PUs with a diversified palette of properties[5]. Many types of products can therefore be synthesized by exploiting this chemistry such as thermoplastic elastomers[6,7], foams[8,9] for thermal insulation or comfort, adhesives[10,11] and coatings[12,13] to cite only the most important ones.

Among the PU family, polyoxazolidones (POxa) that are characterized by 5-membered cyclic carbamate (urethane) linkages have received attention. Their unique chemical inertness, high thermal stability and high glass transition temperature make them ideal candidates for applications as materials requiring high thermal and chemical resistance.[14–20] Unlike conventional PUs, POxa are more challenging to prepare and many of them are found insoluble in common organic solvents, rendering difficult their characterization. As illustrated in Scheme 1a, the most relevant pathway for POxa consists in the polyaddition of diisocyanates with diepoxides at temperature >150-200°C.[21] Under these harsh conditions, the chain propagation was accompanied by major side-reactions causing difficulties to design high molar mass linear polymer chains. These include the thermally favored trimerization of isocyanates into isocyanurates, leading to a deviation of stoichiometry of the reagents and the formation of a cross-linked network.[22] The reactions of isocyanates with some solvents such as DMF to form amidine end-capped POxa chains, or with the catalyst also limited the scope of chemicals that could be used together with the comonomers.[23,24] POxa with

ether linkage defects within their microstructure were formed by two or more consecutive chain enchainments involving the epoxide monomers. It should be noted that the reaction furnished two types of oxazolidone linkages, i.e. 4- and 5-substituted ring, due to the regio-irregular ring-forming step.[24] To surpass these hurdles, Buchmeiser's group developed recently new cooperative catalysts based on a N-heterocyclic carbene and a metal halide to prepare POxa of high molar mass (M_n = 30-50 kg/mol) in sulfolane.[24] However, the process still required high polymerization temperatures (T > 200 °C) and the use of toxic isocyanates. Alternative routes to deliver POxa free of defects under less demanding conditions and without using isocyanates are highly desired. Only few relevant examples can be cited, such as the polycondensation of diurethanes with diepoxides at 90 °C using a tertiary amine as catalyst (Scheme 1b),[14,25] or the copper-catalyzed 4-components reaction between a dialkyne, a diamine, an aldehyde and carbon dioxide at 75-80 °C (Scheme 1c).[26–28] Recently, we reported a novel methodology to fabricate POxa by the facile polyaddition of CO_2-sourced bis(α-alkylidene cyclic carbonate)s (bisαCCs) with a primary diamine (1,8-octanediamine) (Scheme 1d).[29,30] As the α-alkylidene cyclic carbonate group is highly reactive towards aminolysis, the polymerizations occurred at room temperature under catalyst-free conditions, furnishing unprecedented defect-free and regioregular POxa bearing additional pendant hydroxyl groups, named poly(hydroxyoxazolidone)s. Although the proof of concept was validated on a single non-hindered aliphatic primary diamine (1,8-octanediamine), the large diversity of diamines that can potentially be used and the presence of the hydroxyl groups on the polymer backbone easily transformable by chemical modification are offering many unexplored possibilities for the construction of functional polyoxazolidones under mild experimental conditions. Moreover, as the oxazolidone linkage originates from a two-step process, i.e. the regioselective aminolysis of the α-alkylidene cyclic carbonate group into the oxo-urethane function followed by the spontaneous intramolecular cyclization (Scheme 2), we hypothesized that the structure of the polymer might be tuned by selecting the reaction conditions and the chemical structure of the comonomers. For instance, the cyclization might be slowed down by the use of sterically hindered diamines, leading to POxa bearing both oxazolidone and oxo-urethane linkages.

This work aims at establishing a roadmap of the polymerization features and the structural characteristics of the polyoxazolidones regarding the nature of the diamines and the reaction conditions. This will open the access to a library of new regioregular isocyanate-free polyurethanes with hydroxyl functionality and/or pendent ketones under mild reaction conditions. Then, the dehydration of the poly(hydroxyoxazolidone)s will be investigated to afford a novel class of polyoxazolidones with exocyclic vinylene functionality, i.e. poly(alkylidene oxazolidone)s, with remarkable thermal stability. This

work clearly highlights the potential of this simple chemistry for the construction of hydroxyl- or olefinic-functional polyoxazolidones under mild operating conditions.

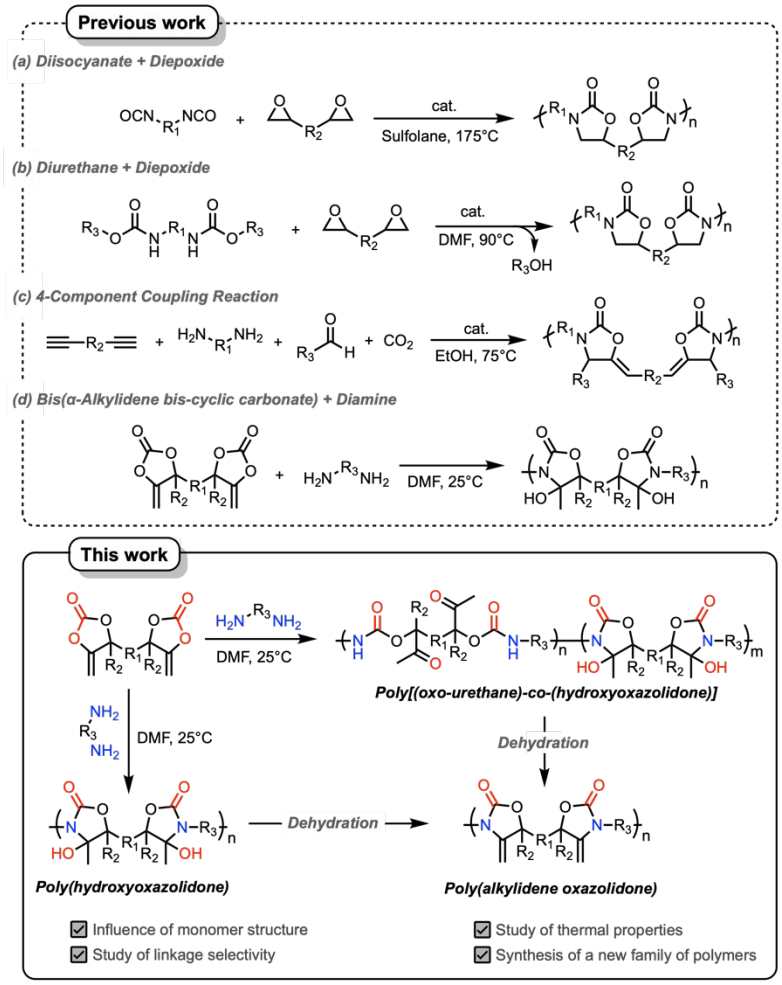

Scheme 1. Main routes towards polyoxazolidones and scope of this work.

Experimental section

Materials.

Potassium hydroxide (85 %) and Sulfuric acid were purchased from Acros Organics. 1,2-Diaminocyclohexane (mixture of isomers, 99 %) and Triethylamine (> 99 %) were purchased from Alfa Aesar. 1,4-Cyclohexanedione (98 %), Cyclohexane-1,4-diamine (mixture of isomers, 99 %), trans-1,4-Diaminocyclohexane (99%) and Zinc iodide (≥ 99 %) were purchased from Fluorochem. 1,8-Diazabicyclo(5.4.0)undec-7-ene (DBU) (99 %)

was purchased from Fluka. 1,8-Diaminooctane (98 %), 2,5-Hexanedione (≥ 98 %), 3-Methyl-3-butyn-2-ol (98 %), 3,3′-Diamino-N-methyldipropylamine (96 %), Aniline (≥ 99.5 %), Benzylamine (≥ 99 %), Copper iodide (≥ 98 %), Cyclohexylamine (> 99 %), Ethynylmagnesium bromide solution (0.5 M in THF), Heptylamine (99%), m-Xylylenediamine (99 %), Phenol (≥ 99 %), Tetrabutylammonium bromide (≥ 98 %) were purchased from Sigma-Aldrich. Hydrochloric acid was purchased from Labotech. 1,2-Bis(2-aminoethoxy)ethane (> 98 %) was purchased from TCI. Glacial acetic acid and ammonium chloride (≥ 99.5 %) were purchased from VWR. Copper iodide was dispersed in acetic acid glacial overnight, filtered, washed with methanol under nitrogen flow, and dried under vacuum.

4,4-dimethyl-5-methylene-1,3-dioxolan-2-one (**αCC**) was synthesized according to the protocol described elsewhere[29]. The two bis(αCC)s monomers, 4,4'-(ethane-1,2-diyl)bis(4-methyl-5-methylene-1,3-dioxolan-2-one) (**αCC1**) and 4,12-dimethylene-1,3,9,11-tetraoxadispiro[4.2.48.25]tetradecane-2,10-dione (**αCC2**) were synthesized according to a procedure described elsewhere.[31]

Characterizations.

Nuclear magnetic resonance (NMR) spectroscopy. ^{1}H-NMR analyses were performed on a Bruker 400 MHz spectrometer at 25 °C in the Fourier transform mode. 16 scans for ^{1}H spectra and 512 scans for ^{13}C spectra were recorded. Cross-polarization magic angle spinning (CP-MAS) solid state ^{13}C-NMR spectra were collected using a Bruker Avance DSX-400 instrument. Samples were packed in 4 mm zirconia rotors and spun at 10 kHz.

Size exclusion chromatography (SEC). Number-average molecular weight (M_n) and dispersity (D) of the polymers were determined by size exclusion chromatography (SEC) in dimethylformamide (DMF) containing LiBr (0.025 M) at 55 °C (flow rate: 1 mL/min) with a Waters chromatograph equipped with three columns (PSS gram 1000Å (x2), 30 Å) and a precolumn, a dual absorbance detector (Waters 2487) and a refractive index detector (Waters 2414).

Thermogravimetric analysis (TGA). TGA analysis was performed on a TGA2 instrument from Mettler Toledo. Around 10 mg of sample was flushed with nitrogen (20 mL/min) for 10 min at 25 °C. The sample was then heated at 20 °C/min until 600 °C under nitrogen atmosphere (20 mL/min).

Dynamic scanning calorimetry (DSC). DSC analysis was performed on a DSC Q2000 differential calorimeter (TA Instruments). All the experiments were performed under ultrapure nitrogen flow. Samples of 5–8 mg were used and placed in sealed aluminum

pans. The samples were first heated at a rate of 10 °C min-1 from 25 °C to 150 °C. Subsequently, the samples were cooled down to -80 °C at a rate of 10 °C/min and then heated to 250 °C at 10 °C/min. The last heating cycle was used for the determination of the T_g.

General procedure for the synthesis of hydroxyoxazolidones by aminolysis of model αCC.

Synthesis protocol for 3-heptyl-4-hydroxy-4,5,5-trimethyloxazolidin-2-one (2a) and 3-benzyl-4-hydroxy-4,5,5-trimethyloxazolidin-2-one (2b). **αCC** (2 g, 15.6 mmol, 1 eq.) was added to a reaction tube containing dichloromethane (4 mL) and the amine (**A1** or **A2)** (15.6 mmol, 1 eq.). The mixture was stirred at 50 °C for 24 h. The product was purified by chromatography onto silica (eluent: dichloromethane then dichloromethane/methanol (50:50)) and collected by evaporation of the solvent under reduced pressure at room temperature for 24 h. ^{1}H- and ^{13}C-NMR and ATR-IR spectra are provided in supporting information (Figures S1-S3, S4-S6).

Synthesis of 3-cyclohexyl-4-hydroxy-4,5,5-trimethyloxazolidin-2-one (2c). **αCC** (2 g, 15.6 mmol, 1 eq.) was added to a reaction tube containing DMF (4 mL) and the amine **A3** (15.6 mmol, 1 eq.). The mixture was stirred at 25 °C for 48 h. The solvent was evaporated and the obtained solid was washed with water on a Buchner apparatus, and dried under reduced pressure at room temperature for 24 h. ^{1}H- and ^{13}C-NMR and ATR-IR spectra are provided in supporting information (Figures S7-S9).

General procedure for the synthesis of poly(hydroxyoxazolidone)s.

The bis(α-alkylidene cyclic carbonate) (**αCC1** or **αCC2**; 0.79 mmol, 1 eq.) was added to a reaction tube containing dry DMF (1.2 mL). The diamine (**AA1**-**AA7;** 1 eq.) was added and the tube was stirred at the specified temperature. After 24 h, an aliquot of the crude product was taken out for SEC and ^{1}H-NMR characterizations. The polymer was purified by precipitation in diethyl ether before filtration and vacuum drying at room temperature overnight.

The structure of the purified polymers was obtained by ^{1}H- and ^{13}C-NMR characterizations. Insoluble polymers were characterized by solid-state ^{13}C-NMR. All NMR characterizations are provided in the supporting information section.

General procedure for the dehydration of poly(hydroxyoxazolidone)s.

The polymer (500 mg) was added to a round bottom flask containing glacial acetic acid (5 mL). The mixture was stirred and refluxed for 2 h at 120 °C. Then, the dehydrated polymer was collected by precipitation in diethyl ether at -20 °C for 24 h before filtration

and vacuum drying for 24 h at room temperature. All NMR characterizations are provided in supporting information.

Results and discussion

In our initial communication highlighting the proof of concept, we introduced the synthesis of poly(hydroxyoxazolidone)s from a bis(αCC) (**αCC1**, Scheme 2) and a single primary diamine, the aliphatic primary 1,8-octanediamine (**AA1**), at room temperature for 24h. To enlarge the scope of the process and get further insights into the microstructural and thermal characteristics of the polymers, we extended the step-growth copolymerization to two bis(αCC)s (**αCC1** and **αCC2**, Scheme 2) with (cyclo)aliphatic and aromatic diamines of different steric hindrance and nucleophilicity such as 1,8-octanediamine **AA1** (as the reference diamine), 1,2-bis(2-aminoethoxy)ethane (Jeffamine EDR-148, **AA2**), 3,3′-Diamino-N-methyldipropylamine (**AA3**), various cyclohexane diamine stereoisomers (**AA4**, **AA5**, and **AA6**) and m-xylylene diamine (**AA7**) (Scheme 2). The cyclohexane diamines stereoisomers and m-xylylene diamine have been selected due to their different stereo-electronic characters, but also because of their possible biorenewable supply from lignin-fractionation and derivatization.[32,33] To understand how the amine may influence the aminolysis rate of α-alkylidene cyclic carbonate and the subsequent cyclization step, model reactions were first investigated on monofunctional organic molecules before implementing the optimal conditions to the polymerization (Scheme 2).

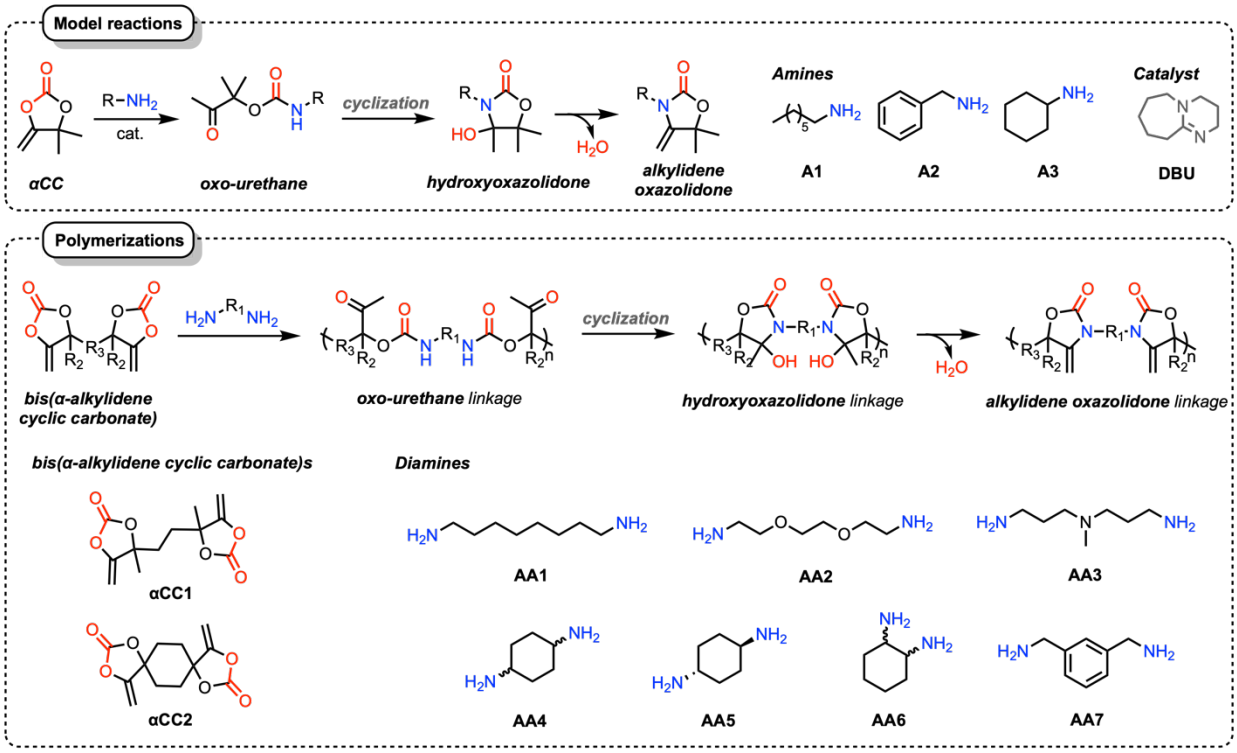

Scheme 2. Substrate scope for the model reaction of **αCC** with several amines and for the polyaddition of bis(α-alkylidene cyclic carbonate)s to diamines.

Model reactions

The DBU-catalyzed aminolysis of the model α-alkylidene cyclic carbonate, 4,4-dimethyl-5-methylene-1,3-dioxolan-2-one (**αCC**), by heptylamine **A1** (as the reference amine), benzylamine **A2** and cyclohexylamine **A3** was first investigated (Scheme 2). The reagents were used in stoichiometric conditions (in order to mimic the polymerization conditions) in DMF (C = 3.90 M) at 25 °C. It should be noted that experiments involving the aromatic amine **A2** were studied in a twice more diluted medium (C = 1.95 M) since the obtained product presented a low solubility in DMF. For a fair comparison of the different amines, this model reaction was also achieved under identical reaction conditions for heptylamine **A1**. The kinetics of the model reactions were monitored by ^{1}H-NMR spectroscopy. All aliquots were quenched by the addition of one drop of acid to protonate the amine before storage at -20 °C.

Figure 1 summarizes both the **αCC** conversion and selectivities for the oxo-urethane **1** and the hydroxyoxazolidone **2** regarding the amine scope (**A1-3**).

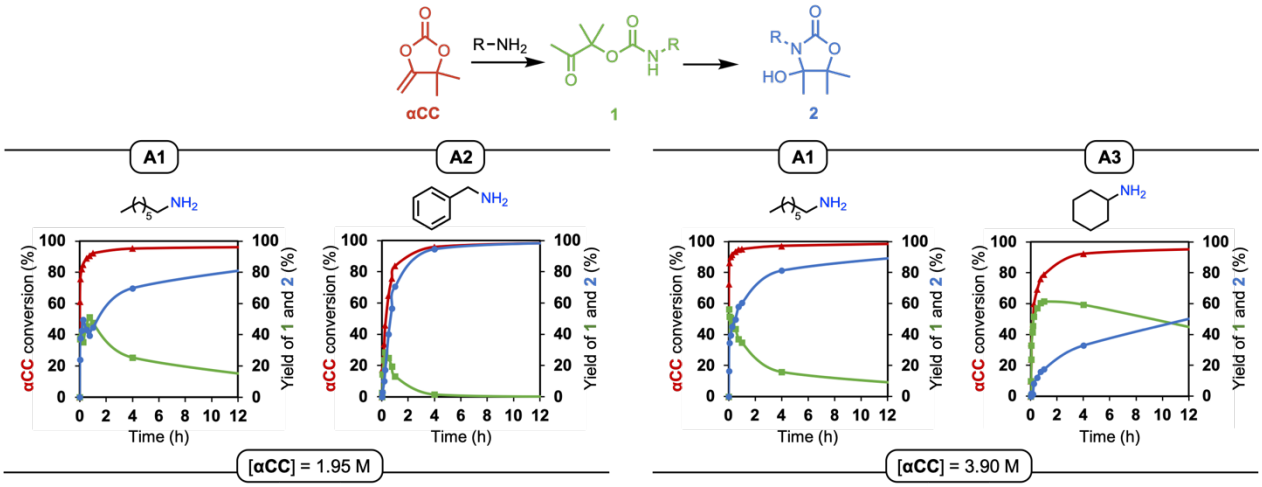

Figure 1. Time evolution of the **αCC** conversion and yields in oxo-urethane **1** and hydroxyoxazolidone **2**. Left: aminolysis of **αCC** with heptylamine (**A1**) or benzylamine (**A2**) in DMF (C = 1.95 M). Right: aminolysis of **αCC** with heptylamine (**A1**) or cyclohexylamine (**A3**) in DMF (C = 3.90 M). Conditions: [αCC]/[NH_2] = 1, 25 °C, no catalyst.

Table 1. Selected kinetic data for the model reaction between **αCC** and the amines **A1**, **A2**, **A3**.

Entry	Amine	[C] (M)	Time	Conversion of **αCC** (%)	Yield for **1** (%)	Yield for **2** (%)	Selectivity for **1** (%)	Selectivity for **2** (%)
1	**A1**	3.90	15 min	92	47	45	51	49
2			24 h	> 99	2	98	2	98
3		1.95	15 min	85	35	50	41	59
4			24 h	97	3	94	3	97
5	**A2**	1.95	15 min	46	27	17	61	39
6			24 h	> 99	0	>99	0	100
7	**A3**	3.90	15 min	60	52	8	87	13
8			24 h	97	97	23	24	76

Conditions: [aCC]/[NH_2] = 1, 25 °C, solvent =DMF, no catalyst.

At 25 °C under catalyst-free conditions, the three amines ring-opened **αCC** with an almost quantitative conversion after 24 h (Table 1). The primary aliphatic amine **A1** was the most reactive, as expected from its more flexible chemical structure, while the cycloaliphatic one **A3** presented the lowest reactivity, probably due to an increased steric hindrance (Figure 1). Indeed, 92 % of **αCC** were converted by reaction with **A1** after only 15 min compared to 60 % with **A3** at identical concentration (C = 3.90 M) (Table 1, entries 1 and 7). The aromatic amine **A2** was less reactive than **A1** affording a moderate conversion of 46 % after 15 min at C = 1.95 M compared to 85 % with **A1** under identical experimental conditions (Table 1, entries 3 and 5). All amine/**αCC** model reactions delivered after 15 min a mixture oxo-urethane **1** and oxazolidone **2**. The **αCC** conversion increased with the reaction time to reach almost completion after 12 h of reaction for **A1** and **A2** (Figure 1). Reaction was slower with **A3** but almost complete after 24h (Table 1). Importantly, the product selectivity progressively evolved with time in all cases (Figure 1), as the consequence of the spontaneous intramolecular cyclization of **1** into **2**, to afford the corresponding oxazolidones with a selectivity of 76 % for **A3**, 98% for **A1** and 100 % for **A2** after 24 h (Table 1).

The careful interpretation of the kinetic studies demonstrated that the oxazolidone ring formation followed a trend in opposition with the **αCC** ring opening upon the nucleophilic attack of the selected amines. Indeed, the ring closure of the oxo-urethane into product **2** was faster using benzyl amine **A2** (Figure 1). The cyclohexylamine **A3** presented the

lowest reactivity for both the ring-opening of **αCC** and the cyclization towards the formation of **2** (Figure 1). These studies highlight that both the electronic effects and the hindered structure of the amine had a strong influence on the rates of the aminolysis and the intramolecular cyclization of the oxo-carbonate intermediate into the oxazolidone.

The effect of the addition of an organobase (DBU) (at a loading of 5 mol%) on the **αCC** conversion and the product selectivity was then evaluated for reactions carried out for 24h at 25°C. DBU was selected as it facilitated the ring-opening of αCC by amines[29], alcohols[29] and thiols[31]. In order to evaluate the influence of DBU on the rate of formation of the oxo-urethane **1** and the hydroxyoxazolidone **2**, the reactions were followed by ^{1}H-NMR spectroscopy for 2 h and the results are collected in Figure 2.

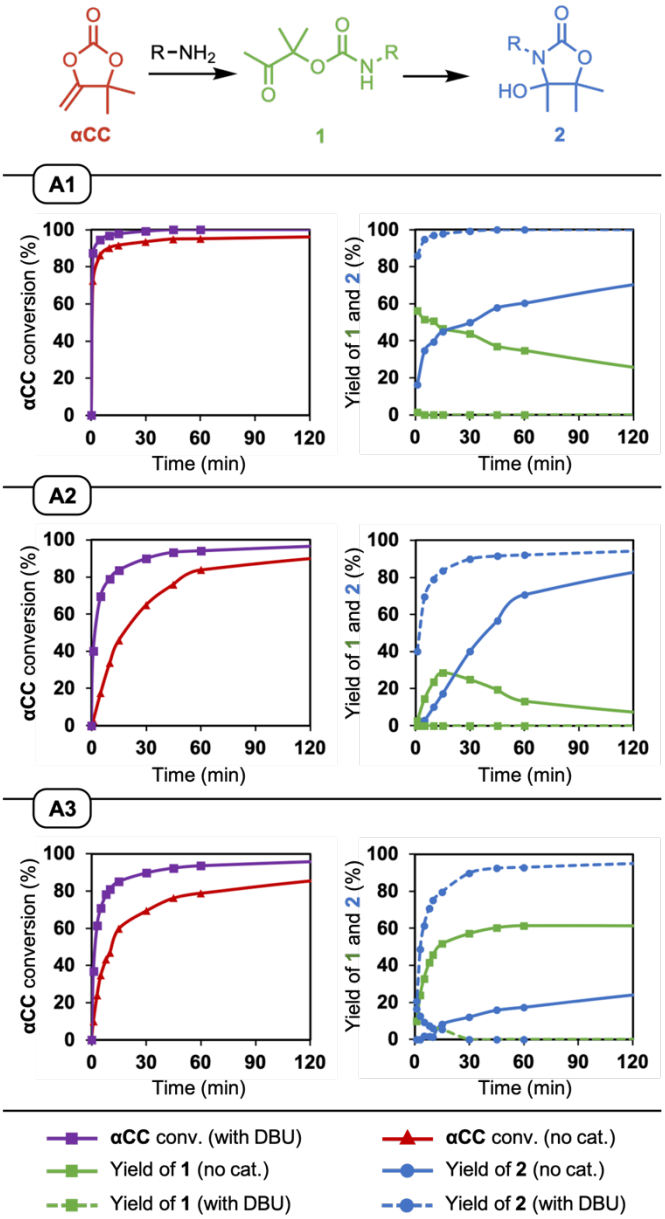

Figure 2. Benchmarking of the time evolution of the **αCC** conversion and yields in oxo-urethane **1** and hydroxyoxazolidone **2** for the aminolysis of **αCC** with the amines **A1-A3** under catalyst-free or DBU driven reactions at 25°C. *Conditions: [αCC]/[NH_2]=1, [αCC]=3.90 M with A1 and A3, or [αCC] = 1.95 M with A2; DMF, 25°C, 5 mol% DBU compared to αCC.*

In all cases, the addition of DBU strongly accelerated both steps of the cascade reactions (Figure 2). For instance, **αCC** was fully reacted with **A1** in only 45 min in the presence of DBU (compared to 24h in the absence of DBU). The catalytic effect of the organobase was much more marked for the less reactive amines **A2** and **A3** with **αCC**

conversions of 85 % or 82% being reached after 15 min with **A3** or **A2**, respectively (compared to 60 % or 46% without catalyst). Besides the organocatalyst had a remarkable catalytic activity on the intramolecular ring formation step and improved the product selectivity. As illustrated in Figure 2, the oxo-urethane **1** was indeed nearly not observed in the presence of the catalyst even at the early stage of the reaction and for the three different amines, which is in sharp contrast to the reactions carried out in the absence of catalyst. Overall, the reactions of **αCC** with the different amines (**A1**, **A2**, **A3**) illustrate the versatility and applicability of the methodology that is able to deliver oxazolidones with a yield close to 100 % in less than 2 h.

Dehydration of hydroxyoxazolidones

The presence of a tertiary alcohol in the chemical structure of the hydroxyoxazolidones makes these latest suitable candidates to deliver oxazolidones with exocyclic vinylene functionality by dehydration. The optimization of the reaction on model compounds is a then prelude to the fabrication of functional poly(α-alkylidene-oxazolidone)s by dehydration of the parent poly(hydroxyoxazolidone)s. The substrate scope was first enlarged by synthesizing, isolating and purifying three hydroxyoxazolidones **2a**, **2b**, and **2c** (Scheme S5) by the reaction between **αCC** and **A1**, **A2** or **A3** following procedures discussed above (see experimental section 1).

Inspired by the literature,[34] the dehydration of the hydroxyoxazolidones **2a-c** was realized in refluxing glacial acetic acid (HAc), a cheap, non-toxic, readily available and biorenewable reagent. The dehydration of **2** into the corresponding α-alkylidene oxazolidone **3** (Scheme 3) was monitored by ^{1}H-NMR spectroscopy (see ESI). Excellent dehydration yields of 92 to 100 % were obtained for all substrates, including the more sterically hindered product **2c**, with the selective formation of the corresponding α-alkylidene oxazolidone **3**.

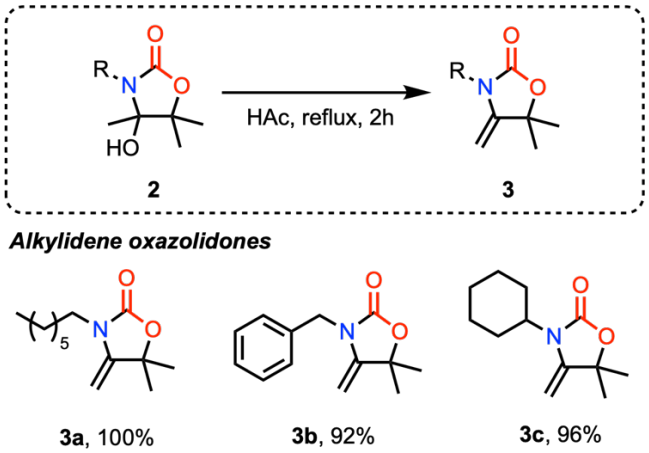

Scheme 3. Substrate scope of hydroxyoxazolidones dehydration into α-alkylidene oxazolidones.

Conditions: [O]=0.22 M in glacial acetic acid, 120 °C, 2 h.

Synthesis of poly(hydroxy-oxazolidone)s

The polyaddition of two CO_2-sourced bis(α-alkylidene cyclic carbonate)s (bisαCCs; **αCC1** and **αCC2**) with 7 different diamines (**AA1** – **AA7**) was then considered (Scheme 2) with the aim to elucidate the influence of the comonomer structures on the polymerization course. This facile polyaddition approach was expected to provide a library of new polyurethanes. It has to be noted that alike poly(oxazolidone)s made from diisocyanates and diepoxides, some of our poly(hydroxyoxazolidone)s displayed poor or no solubility in common organic solvents. Therefore, for insoluble polymers, their molecular parameters (M_n, M_w/M_n) could not be determined by size-exclusion chromatography (SEC). Their microstructural characterization was also difficult and could be elucidated by ^{13}C-solid state NMR spectroscopy only.

Polymerizations under ambient and catalyst-free conditions. Polymerizations were first carried out at 25 °C in DMF for 24 h without any catalyst. Table 2 summarizes the conversion of the bisαCCs, determined by ^1H-NMR spectroscopy and the selectivity for the oxo-urethane and oxazolidone linkages. The macromolecular parameters of the chains are also included and were determined by SEC on the crude reaction medium to avoid any fractionation of the polymers during precipitation.

Table 2. Conversions, molecular characteristics and linkages selectivity for polymers obtained by the polyaddition of bisαCCs with diamines after 24 h at 25 °C in DMF (the structure of the monomers is illustrated in Scheme 2).

Entry	Polymer	Monomers			Polymer characteristics				
		BisαCC	Diamine	Conv. (%)[a]	M_n (g/mol)[b]	M_w (g/mol)[b]	D[b]	Oxo-urethane linkage (%)	Oxazolidone linkage (%)
1	**P(CC1-AA1)**	**αCC1**	**AA1**	> 99	24,900,	44,800	1.8	/	100
2	**P(CC1-AA2)**		**AA2**	> 99	4,200	8,400	2.0	/	100
3	**P(CC1-AA3)**		**AA3**	>99	20,400	36,100	1.8	/	100
4	**P(CC1-AA4)**		**AA4**	> 99	3,000	4,700	1.6	32	68
5	**P(CC1-AA5)**		**AA5**	> 99	--[c]	--[c]	--[c]	N.Q.[d]	N.Q.[d]
6	**P(CC1-AA6)**		**AA6**	N.d.	500	400	1.4	14	86
7	**P(CC1-AA7)**		**AA7**	> 99	4,000	7,600	1.9	/	100
8	**P(CC2-AA1)**	**αCC2**	**AA1**	> 99	--[c]	--[c]	--[c]	/	100
9	**P(CC2-AA2)**		**AA2**	> 99	--[c]	--[c]	--[c]	/	100
10	**P(CC2-AA5)**		**AA5**	> 99	--[c]	--[c]	--[c]	N.Q.[d]	N.Q.[d]
11	**P(CC2-AA7)**		**AA7**	> 99	--[c]	--[c]	--[c]	/	100
12	**P(CC2-AA6)**		**AA6**	N.d.	--[c]	--[c]	--[c]	/	100

Conditions: [BisaCC] = 0.67 M in DMF, 25 °C, 24 h, no catalyst.

[a]conversion in cyclic carbonate determined by ^{1}H-NMR in DMSO-d_6. N.d. not determined.

[b]determined on the crude product by SEC in DMF/LiBr by using a PS calibration.

[c]not determined due to polymer insolubility in DMF/LiBr and THF.

[d] N.Q.: not quantified. For P(CC1-AA5) and P(CC2-AA5), the solid-state ^{13}C-NMR-spectrum evidenced the presence of the two types of linkages but they could not be quantified.

The bisαCCs conversions were high (> 99 %) in all cases, except for the polymerization carried out with the cycloaliphatic vicinal diamine **AA6** (Table 2, entry 6). In this latter case, the conversion could not be accurately measured due to some peak overlapping.

With **αCC1**, the polymerization medium remained homogeneous all along the span of the reaction, except for **P(CC1-AA5)** synthesis with a polymer that precipitated during its formation. With **αCC2**, the polymer chains precipitated during their formation and were insoluble in common solvents for SEC analysis (THF or DMF/LiBr) or other common organic solvents (DMF, DMSO, DMAc, THF, chloroform, sulfolane, etc.). Only **P(CC2-AA2)** displayed solubility in DMSO which allowed its characterization by liquid-state NMR.

The reference polymer, **P(CC1-AA1),** and the tertiary amine functionalized one, **P(CC1-AA3)**, displayed similar molecular characteristics with relative number average molar masses (M_n) around 20,000 to 25,000 g/mol and a dispersity of 1.8 (Table 2). Figure 3 shows the SEC chromatograms evolution for samples taken at different reaction times (1 min, 1h and 24h) for these two polymerizations. In both cases, SEC chromatograms shifted towards the lower elution time and thus higher molar masses with the polymerization time, as expected for a step-growth type process. Molecular characteristics (M_n, M_w, dispersity D) of the different samples are summarized in Table 3. All other polymers made from **αCC1** presented lower M_n values (Table 3). However, because the molar masses were determined based on a PS calibration and the hydrodynamic volume of the polymers are expected to be different to each other, the molar masses given by SEC analysis are relative and the values cannot be compared. We have also to note that the dispersities were rather low for a step-growth polymerization process (they should be around 2), especially for sample **P(CC1-AA6**) which is due to its oligomeric structure constituted of dimers and trimers (Figure S42). The low M_n obtained for **P(CC1-AA6**) was assumed to be the consequence of a low monomer conversion originating from the high steric hindrance that had to be overcome to increase the polymer chain length or to some side reactions occurring during the process. Further experiments would be required for drawing more conclusions regarding this specific case.

Table 3. Temporal evolution of molecular characteristics during polymerization for **P(CC1-AA1)** and **P(CC1-AA3)**.

Entry	Polymer	Time	M_n (g/mol)[b]	M_w (g/mol)[b]	D[b]
1		1min	4,200	5,600	1.3
2	**P(CC1-AA1)**	1h	11,700	19,800	1.7
3		24h	24,900	44,800	1.8
4		1min	2,700	5,100	1.8
5	**P(CC1-AA3)**	1h	11,600	17,900	1.5
6		24h	20,400	36,100	1.8

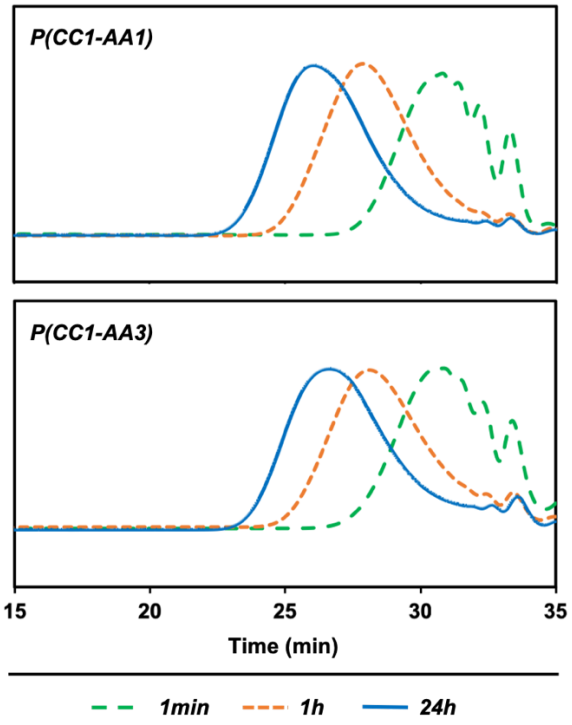

Figure 3. Temporal evolution of SEC chromatograms during the formation of **P(CC1-AA1)** and **P(CC1-AA3)**.

The structure of all polymers prepared from **αCC1** was elucidated by ^{1}H- and ^{13}C-NMR spectroscopies on purified products. As expected from the model reactions, the microstructure of polymers synthesized from the primary aliphatic or aromatic diamines **AA1**, **AA2**, **AA3** and **AA7** contained exclusively hydroxyoxazolidone linkages as

highlighted by the presence of the typical signal of the alcohol pendant group (δ = 6-6.25 ppm) (Figure 4). All the other signals were also characteristic of the targeted polymer structure. ^{13}C-NMR spectra confirmed the formation of poly(hydroxyoxazolidone)s by the typical carbonyl resonance of oxazolidone linkage (δ = 157 ppm) and the two quaternary carbon atoms from the ring structure (δ = 87 and 91 ppm) (Figure 5). All peaks assignments were confirmed by HSQC and HMBC analyses (Figures S16-S18 for **P(CC1-AA1)**, Figures S19-S21 for **P(CC1-AA2)**, Figures S22-S24 for **P(CC1-AA3)**, Figures S29-S30 for **P(CC1-AA6)**, Figures S31-S32 for **P(CC1-AA7)**).

Importantly, it was found that hydroxyoxazolidones and oxo-urethane linkages coexisted within the skeleton of the polymers prepared from vicinal and 1,4-cyclohexanediamine isomers (**AA4**, **AA5**, **AA6**) (Figure 4-d for **P(CC1-AA4)**, Figure 5-d for **P(CC1-AA5)**, Figure 4-e for **P(CC1-AA6)**). The hydroxyoxazolidones/oxo-urethane selectivity in each polymer was determined by ^{1}H-NMR spectroscopy. The selectivity toward each moiety was not determined for **P(CC1-AA5)** due to its lack of solubility. The polymer **P(CC1-AA4**) was constituted by 68 mol% of the hydroxyoxazolidone moiety and 32 mol% of the oxo-urethane unit. Polymer **P(CC1-AA6)** found to contain 14 mol% of oxo-urethane linkage. The presence of the oxo-urethane linkages was due to the cyclization step (transformation of oxo-urethane into oxazolidone) that was slower when sterically hindered amines were used, in line with the model reactions (aminolysis of α**CC** with cyclohexylamine **A3**, Figure 1).

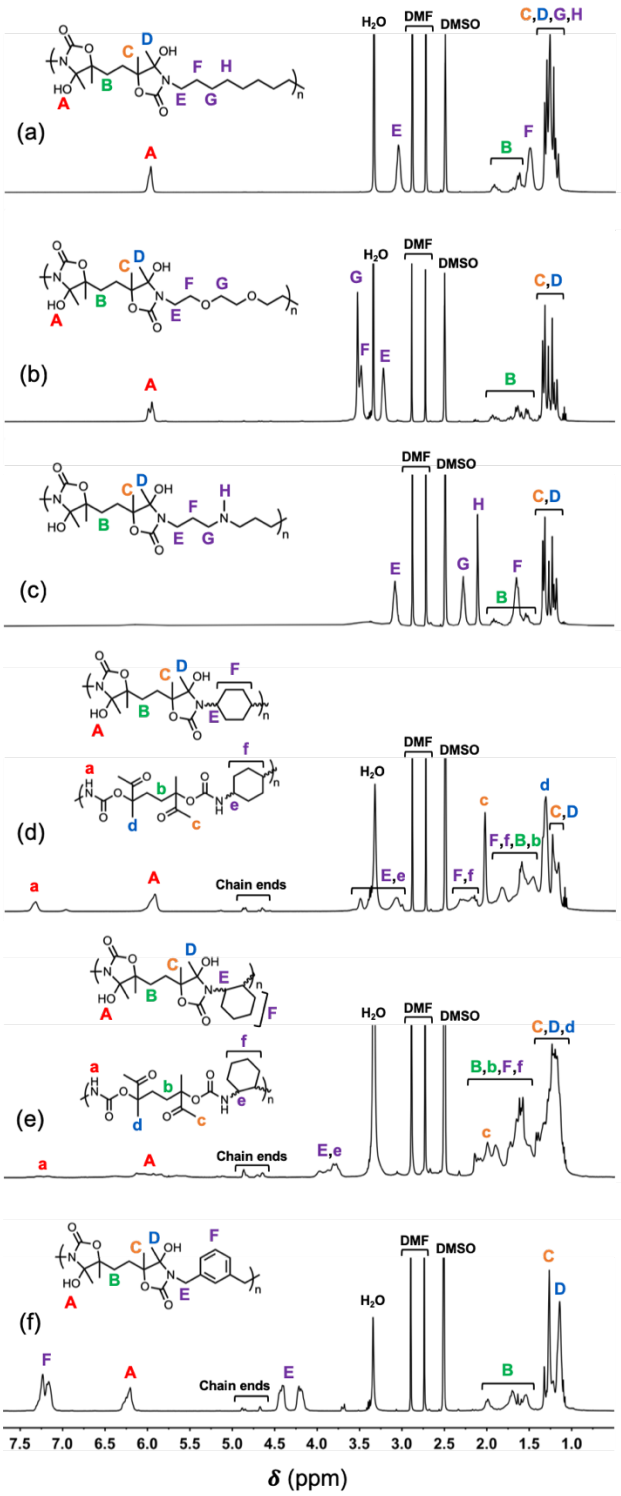

Figure 4. Stacked ^{1}H-NMR spectra of (a) **P(CC1-AA1)** (Table 2, entry 1), (b) **P(CC1-AA2)** (Table 2, entry 2), (c) **P(CC1-AA3)** (Table 2, entry 3), (d) **P(CC1-AA4)** (Table 2,

entry 4), (e) **P(CC1-AA6)** (Table 2, entry 6) and (f) **P(CC1-AA7)** (Table 2, entry 7) in DMSO-d_6 (after purification).

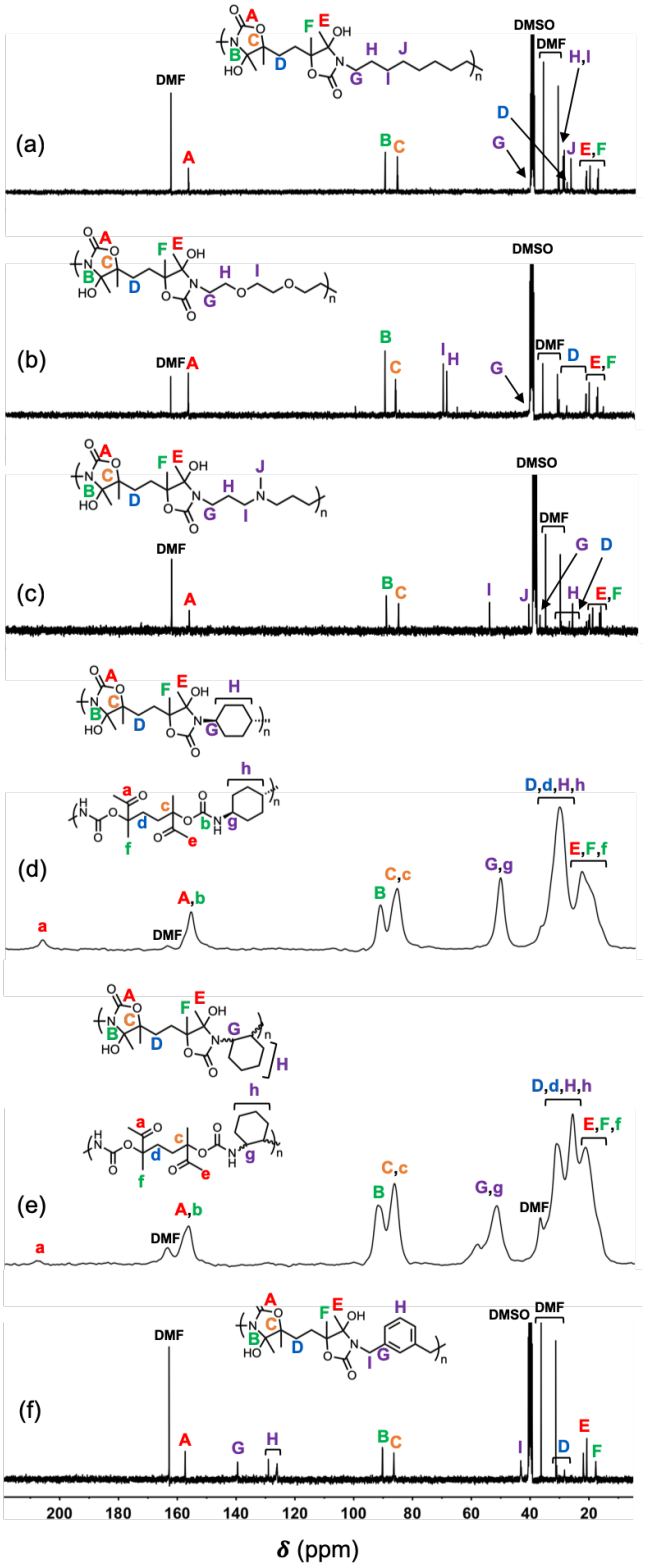

Figure 5. Stacked ^{13}C-NMR and solid-state ^{13}C-NMR spectra of (a) **P(CC1-AA1)** (Table 2, entry 1), (b) **P(CC1-AA2)** (Table 2, entry 2), (c) **P(CC1-AA3)** (Table 2, entry 3), (d) **P(CC1-AA5)** (Table 2, entry 5), (e) **P(CC1-AA6)** (Table 2, entry 6) and (f) **P(CC1-AA7)** (Table 2, entry 7) in DMSO-d_6 (after purification).

The structural identification of insoluble polymers prepared from **αCC2** was realized by solid-state ^{13}C-NMR spectroscopy (Figure 6). At the exception of **P(CC2-AA5)**, all polymers displayed only 100 % of oxazolidone-type linkages, at least within the detection limit of the solid ^{13}C-NMR spectroscopy. The characteristic carbonyl resonances of the oxazolidone group (δ = 155-160 ppm) and the two quaternary carbon atoms of the hydroxyoxazolidone ring structure (δ = 80-87 ppm and 87-95 ppm) were clearly observed in all samples, as well as all other carbon atoms, in line with the proposed structures. The oxo-urethane linkage content was very low or close to zero since no signal characteristic of a ketone group at 210 ppm was observed in solid state ^{13}C-NMR. As previously observed for the polymers prepared from **αCC1**, the polymer prepared from **αCC2** and the 1,4-cyclohexanediamine isomer **AA4** was characterized by hydroxyoxazolidones and oxo-urethane linkages, resulting from a partial intramolecular cyclization of oxo-urethane moieties. It was however not possible to quantify the amount of each moiety in the polymer structure since the solid-state ^{13}C NMR technique does not allow a quantitative analysis.

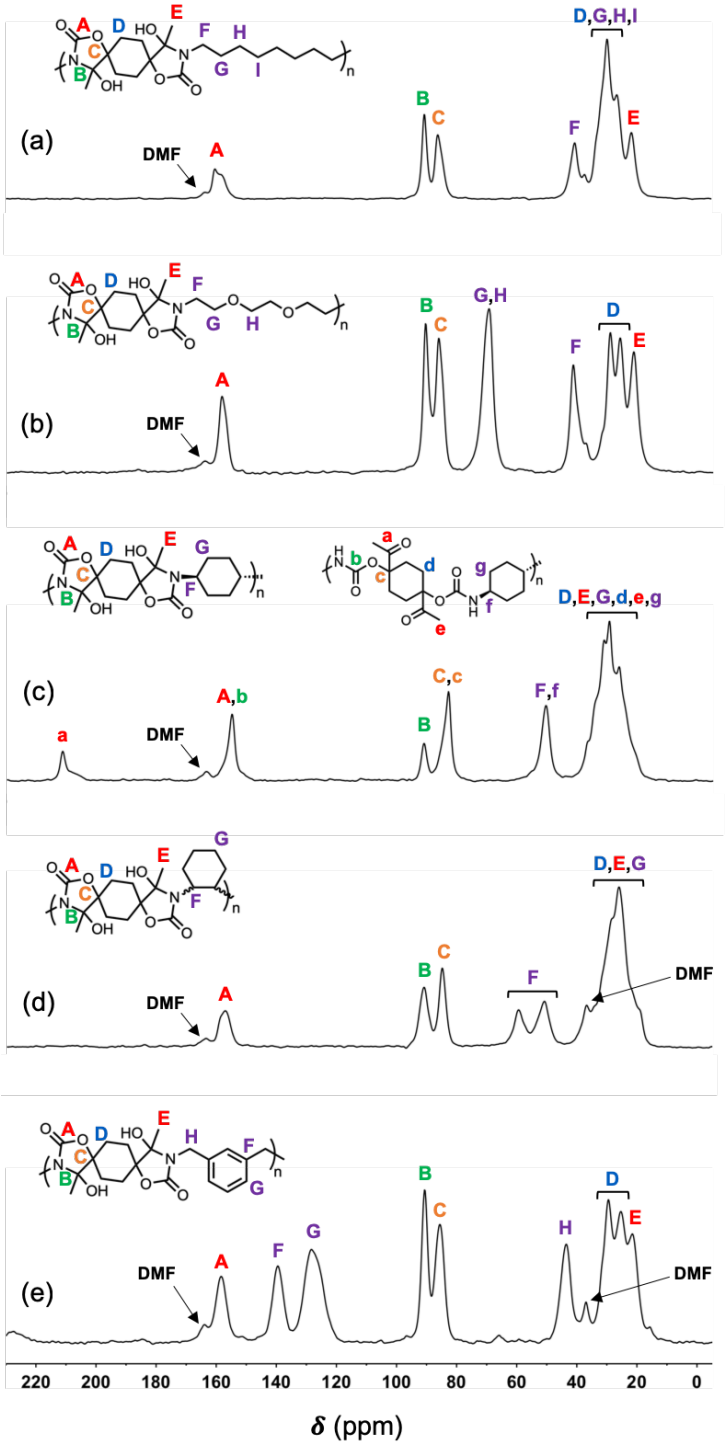

Figure 6. Stacked solid-state ^{13}C NMR spectra of (a) **P(CC2-AA1)**, (b) **P(CC2-AA2)**, (c) **P(CC2-AA5)**, (d) **P(CC2-AA6)**, (e) **P(CC2-AA7)** (after purification).

Polymerizations using a catalyst and/or at higher temperatures. We then evaluated the impact of the DBU catalyst or the temperature (T = 25 or 80 °C) on the polymerization of bisαCC with the diamines on the macromolecular characteristics of the polymers. Since the polymers synthesized from **αCC2** were insoluble in all tested organic solvents, this study was conducted with **αCC1** only and with some of the amines **AA2**, **AA4** and **AA7** that provided soluble polymers at high yield. Results for the polymerizations carried out for 24 h are summarized in Table 4.

Table 4. Conversions and molar masses of polymers prepared by copolymerization of **αCC1** with various diamines with or without DBU and at different temperatures.

Entry	BisαCC	Diamine	T (°C)	Catalyst	Conv. (%)[a]	M_n (g/mol)[b]	M_w (g/mol)[b]	D^b
1			25	--	> 99	4,200	8,400	2.0
2		**AA2**	80	--	> 99	7,500	17,200	2.2
3			25	DBU	> 99	15,500	25,500	1.7
4			25	--	> 99	3,000	4,700	1.6
5	**αCC1**	**AA4**	80	--	> 99	--[c]	--[c]	--[c]
6			25	DBU	> 99	--[c]	--[c]	--[c]
7			25	--	> 99	4,000	7,600	1.9
8		**AA7**	80	--	> 99	--[c]	--[c]	--[c]
9			25	DBU	> 99	--[c]	--[c]	--[c]

Conditions: [αCC1] = 0.67 M in DMF, 24 h, no catalyst or DBU (5 mol%).

[a]conversion in cyclic carbonate determined by ^{1}H NMR in DMSO-d_6. N.d. not determined.

[b]determined on crude products by SEC in DMF/LiBr and by using a PS calibration.

[c]not determined due to polymer insolubility in DMF/LiBr and THF.

By increasing the temperature from 25 to 80 °C, the molar mass of the polymer formed from **AA2** was almost doubled with a molar mass of 7,500 g/mol (compared to 4,200 g/mol at 25 °C) (Table 4, entries 1-2). The use of DBU (5 mol%) at 25 °C had a huge influence on the polymer molar mass that was strongly increased to 15,500 g/mol (Table 4, entry 3). It seemed that the use of a catalyst was the best option for accelerating the growth of the polymer chains, and thus for providing longer polymer chains.

When **AA4** and **AA7** were concerned, the addition of DBU or the increase of the temperature furnished polymers that precipitated during the polymerization and that were insoluble in the solvent used for SEC analysis. This was in sharp contrast to the same polymerizations carried out without DBU at rt that yielded soluble polymers in the reaction medium. These observations suggested that the molar mass of the polymer prepared in the presence of DBU at 25 °C or at 80 °C without DBU were higher than that noted at 25 °C without DBU, and exceeded the solubility limit of the product in DMF (Table 4, entries 5-6 and 8-9). In order to give any clue to this hypothesis and that a possible modification of the chemical structure of the polymer was not responsible for this lack of solubility, we analyzed the polymer **P(CC1-AA7)** prepared under the different reaction conditions (rt without catalyst, rt with DBU, and 80°C without DBU) by solid-state ^{13}C-NMR spectroscopy under identical conditions. (Note here that solid state NMR was required because the polymers prepared with DBU or at higher temperature were insoluble in many organic solvents). Figure S41 confirmed that increasing the temperature or adding a catalyst had no impact on the polymer microstructure, the NMR spectra being identical. The difference of solubility of the polymers synthesized under the different conditions was therefore assigned to a higher molar mass when DBU or a higher temperature was employed for their synthesis, and is not due to a different chemical structure.

Dehydration of poly(hydroxy-oxazolidone)s

The dehydration of poly(hydroxyoxazolidone)s was tested on polymers soluble in common organic solvents, thus on **P(CC1-AA1)**, **P(CC1-AA2)**, **P(CC1-AA4)** and **P(CC1-AA7)**. Polymers were dispersed in glacial acetic acid and the mixture was refluxed at 120 °C for 2 h.

Table 5. Dehydration of poly(hydroxyoxazolidone)s into poly(alkylidene oxazolidone)s. Macromolecular parameters of the polymers before and after dehydration, and selectivity for the two linkages **D1** and **D2** of the dehydrated polymers.

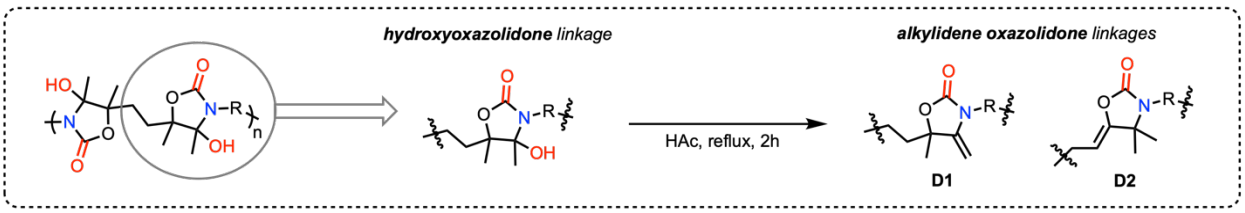

Entry	Polymer	R	M_n (g/mol)[b]	M_w (g/mol)[b]	D[b]	Polymer linkages

1	**P(CC1-AA1)**	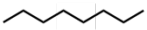	79,200	157,900	2.0	
2	**P(CC1-AA1)D**		36,700	68,300	1.9	**D1**/**D2**: 58/42
3	**P(CC1-AA2)**	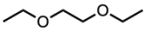	15,900	26,200	1.6	
4	**P(CC1-AA2)D**		4,600	8,700	1.9	**D1**/**D2**: 50/50
5	**P(CC1-AA4)**		3,000	5,200	1.7	
6	**P(CC1-AA4)D**		2,400	4,100	1.7	**D1**/**D2**: 100/0
7	**P(CC1-AA7)**	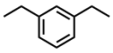	7,200	18,500	2.6	
8	**P(CC1-AA7)D**		4,300	9,000	2.1	**D1**/**D2**: 100/0

The structure of the novel polymers was elucidated by ^{1}H- and ^{13}C-NMR spectroscopies on the purified products (Figures 7-8). The less sterically hindered poly(hydroxyoxazolidone)s, **P(CC1-AA1)** and **P(CC1-AA2)**, were completely dehydrated into the unsaturated poly(oxazolidone) with the formation of the expected α-alkylidene oxazolidone linkage **D1** but also a second linkage **D2** (β-alkylidene oxazolidone) (Table 5). Typical signals for the unsaturated poly(oxazolidone) were indeed identified by the two non-equivalent olefinic protons (δ = 4.10-4.30 ppm) for the linkage **D1** and the olefinic proton associated to **D2** (δ = 4.50-4.70 ppm), in accordance with the chemical shift of similar structures studied in a previous study on small molecules[35]. The complete disappearance of the hydroxyoxazolidone alcohol group (δ = 6 ppm) attested for the completeness of the reaction. ^{13}C-NMR spectrum also showed the appearance of the typical olefinic signals (δ = 82 ppm and 148 ppm for **D1**, δ = 100 ppm and 141 ppm for **D2**) (Figure 8). All these assignments were confirmed by HSQC and HMBC analyses (Figure S33-S40). This **D2** linkage was observed in large amount after dehydrating the sterically unhindered polymers **P(CC1-AA1)** (**D1**/**D2** = 58/42) and **P(CC1-AA2)** (**D1**/**D2** = 50/50). The dehydration of the bulkier poly(hydroxyoxazolidone)s **P(CC1-AA3)** and **P(CC1-AA6)** was also successful and complete. Importantly, the exclusive formation of α-alkylidene oxazolidone linkages **D1** was observed in these two cases.

It is suggested that the **D2** linkage resulted from the carbocation 1,2-Wagner-Meerwein-type rearrangement to yield a more substituted alkene (Scheme 4). This rearrangement was not observed in the model reactions where both alkenes would have the same substitution number. The spontaneous methyl shift might thus be promoted for polymers made up from sterically unhindered diamines. Although further investigations are needed, the presence of a bulky group (such as cycloaliphatic or aromatic group) seemed to prevent this methyl shift.

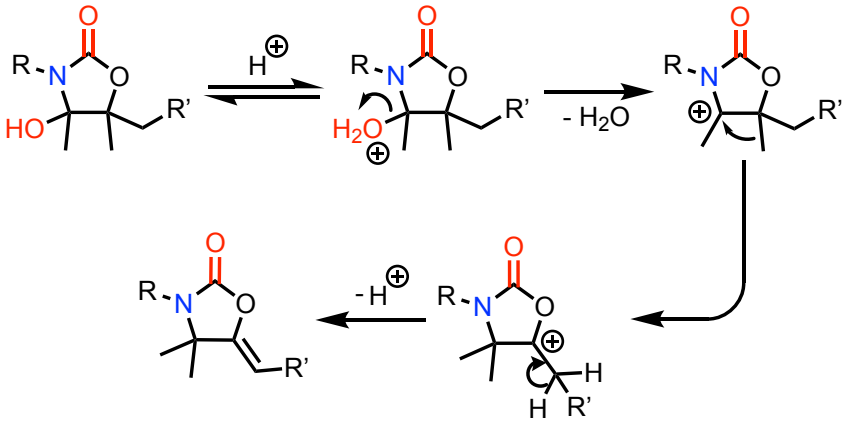

Scheme 4. Proposed mechanism for the dehydration of hydroxyoxazolidones through a Wagner-Meerwein rearrangement.

The molecular parameters of the polymers before and after dehydration are collected in Table 5. The dehydrated polymers had lower apparent M_n than the starting poly(hydroxyoxazolidone)s. However, the chemical structure of the polymers was different and these relative molar masses values could not be compared as the hydrodynamic volume of the polymers was expected to be different in the solvent used for SEC analysis. Note here that the M_n of the starting products (poly(hydroxyoxazolidone)s) were higher than those reported in Table 2 because the polymers were purified by precipitation before performing the dehydration reaction (in Table 2, crude polymers were analyzed). Some fractionation was thus occurring during purification, explaining the higher M_n observed.

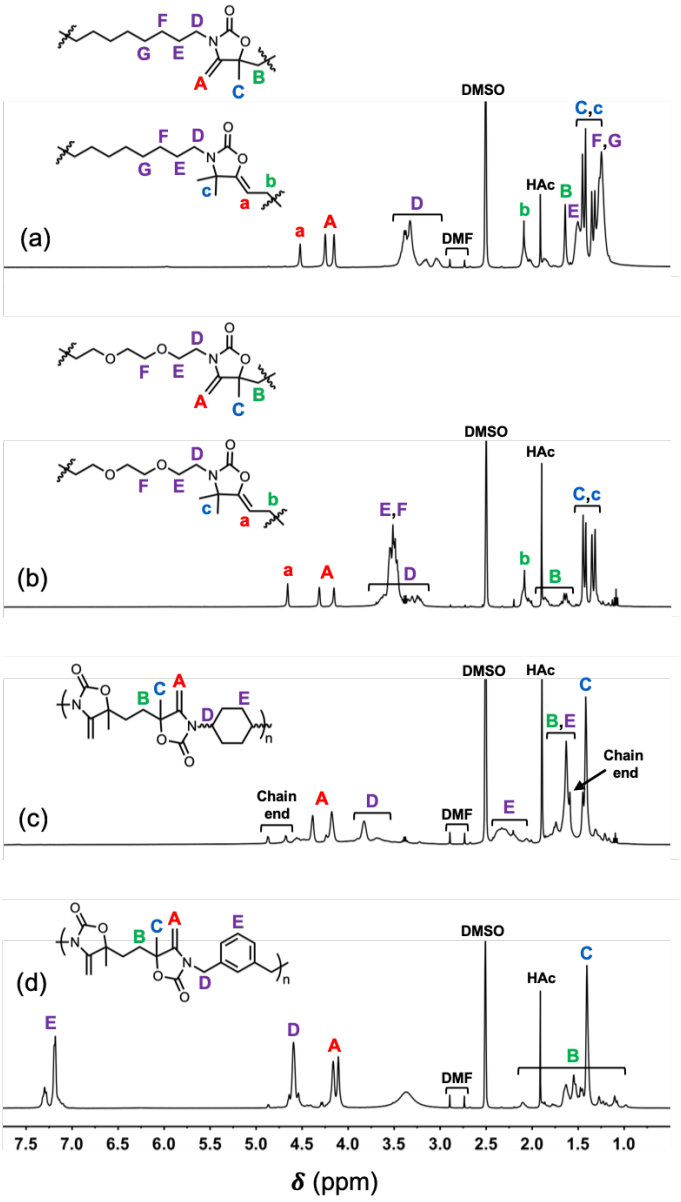

Figure 7. Stacked ^{1}H-NMR spectra of (a) **P(CC1-AA1)D** (Table 5, entry 2), (b) **P(CC1-AA2)D** (Table 5, entry 4), (c) **P(CC1-AA4)D** (Table 5, entry 6) and (d) **P(CC1-AA7)D** (Table 5, entry 8) in DMSO-d_6 (after purification).

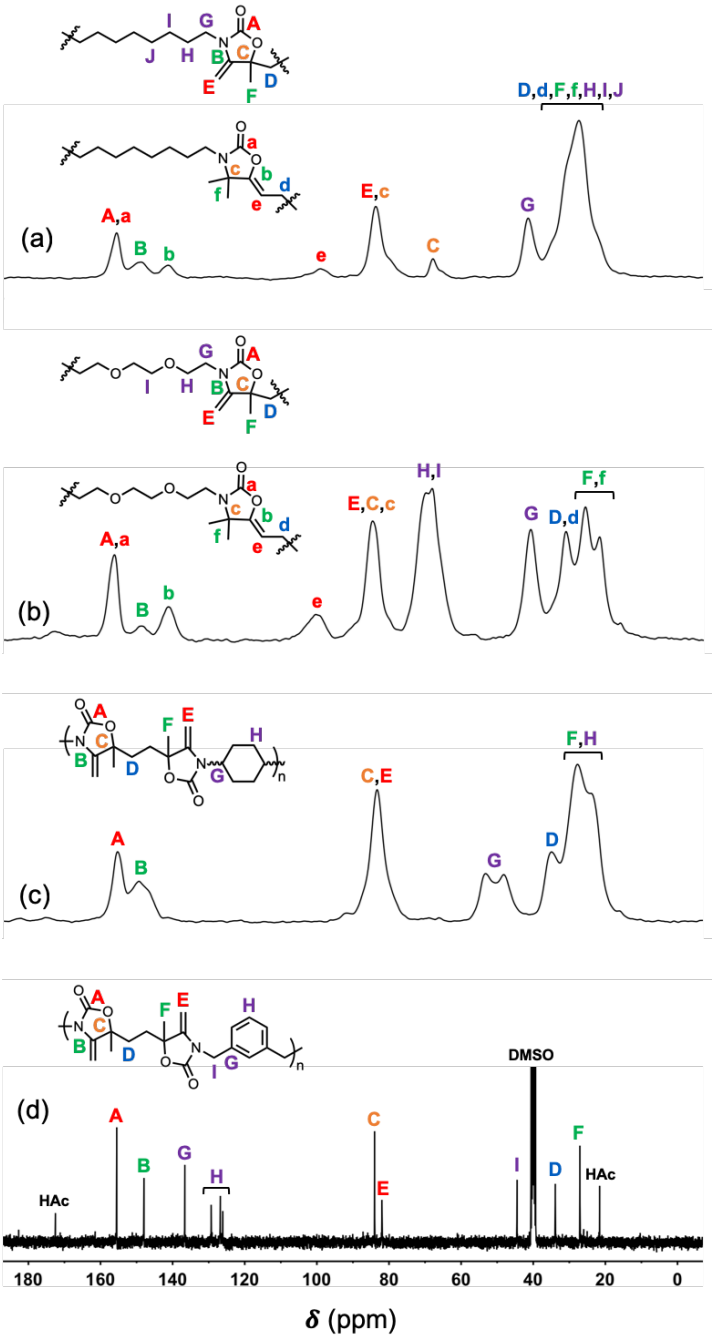

Figure 8. Stacked ^{13}C-NMR and solid-state ^{13}C-NMR spectra of (a) **P(CC1-AA1)D** (Table 5, entry 2), (b) **P(CC1-AA2)D** (Table 5, entry 4), (c) **P(CC1-AA4)D** (Table 5, entry 6) and (d) **P(CC1-AA7)D** (Table 5, entry 8) in DMSO-d_6 (after purification).

Thermal properties of the polymers

The thermal degradation temperature at 10 wt% loss ($T_{d,10\%}$) of the polymers was evaluated by thermogravimetric analysis (TGA) and all data are summarized in Table 6. A multistep degradation pattern was observed for all studied poly(hydroxyoxazolidones)s (Figure 9). The first mass loss at around 150 °C was the result of the evaporation of residual DMF that was impossible to completely remove after polymer synthesis and purification. The second main degradation appeared at around 275 °C for all polymers and was followed by a more important degradation at around 400 °C.

Importantly, TGA analyses of the dehydrated polymers, the poly(alkylidene oxazolidone)s, presented a single degradation pattern at high temperature ($T_{d,10\%}$ = 370-400 °C) (the small mass loss at around 150 °C corresponded to the evaporation of residual acetic acid), highlighting the high thermal stability of the polymer. This $T_{d,10\%}$ was similar to that measured for the final degradation pattern of the parent poly(hydroxyoxazolidone)s. Although additional experiments would be required, this suggests that the first degradation step of poly(hydroxyoxazolidone) corresponded to the dehydration of the polymer with the formation of the poly(alkylidene oxazolidone). Additionally, the poly(hydroxyoxazolidone) **P(CC1-AA7)** and poly(alkylidene oxazolidone) **P(CC1-AA7)D** prepared from m-xylylene diamine provided some char at 600 °C, 13.5 and 12.6 wt% respectively (after subtracting the content of residual solvent trapped in the polymer).

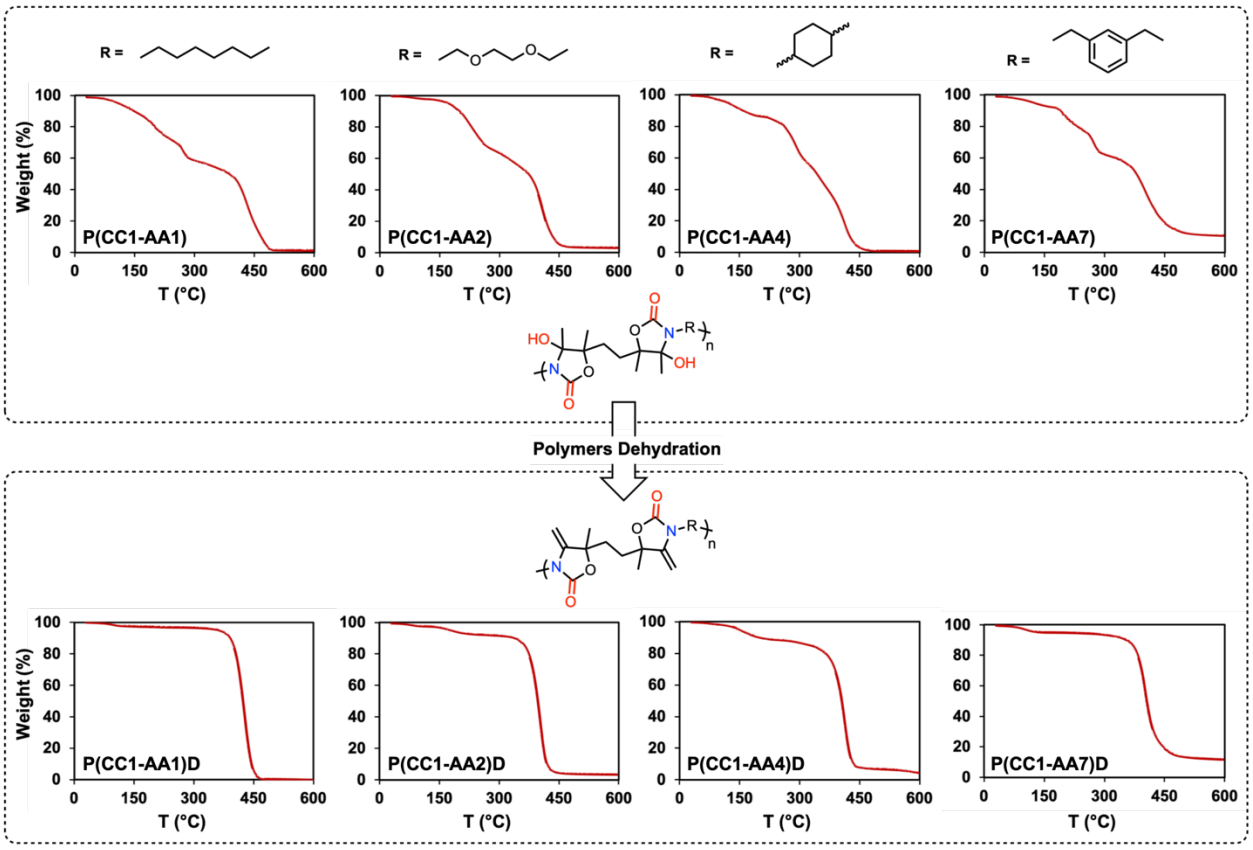

Figure 9. TGA curves for the polymers **P(CC1-AA1)**, **P(CC1-AA2)**, **P(CC1-AA4)** and **P(CC1-AA7)** (top) and their respective dehydrated product (bottom).

We then analyzed the polymers by dynamic scanning calorimetry (DSC) to evaluate the glass transition temperature (T_g) of the polymers. Due to solvent evaporation and probably the thermal-induced dehydration of the poly(hydroxyoxazolidone)s, we were not able to determine their T_g. However T_g values were obtained for the dehydrated polymers **P(CC1-AA1)D** (T_g = 89 °C) and **P(CC1-AA7)D** (T_g = 130 °C) (Table 6). The highest T_g was measured for the polymer prepared from m-xylylene diamine **AA7**. No melting temperature was observed under the investigated conditions. Despite their clean TGA pattern, polymers **P(CC1-AA2)D** and **P(CC1-AA4)D** did not provide exploitable data by DSC and no glass transition or melting temperatures were determined for these polymers.

Table 6. Degradation temperature and glass transition temperature determined by TGA and DSC analyses for the dehydrated polymers.

Entry	Polymer	$T_{d,10\%}$ (°C)	T_g (°C)
1	**P(CC1-AA1)D**	397	89
2	**P(CC1-AA2)D**	370	N.d.
3	**P(CC1-AA4)D**	367	N.d.
4	**P(CC1-AA7)D**	375	130

N.d. could not be determined.

Conclusion

This work described the synthesis and the characterization of novel poly(oxazolidone)s by polyaddition of CO_2-sourced bis(α-alkylidene cyclic carbonate)s (bisαCCs) with various di-primary amines, with the objective to study the influence of the reaction conditions on the structure and macromolecular parameters of the polymers. Model reactions on small molecules were first performed in order to understand the impact of the structure of the amine on the rate, yield and selectivity of the reactions. The amine structure showed to have an influence on the rates of reaction for both the ring-opening of the cyclic carbonate and the intramolecular cyclization of the oxo-urethane intermediate into the hydroxyoxazolidone. Aliphatic and benzylic amines provided mainly the hydroxyoxazolidone, thus the intramolecular cyclization of the oxo-urethane was fast. Cycloaliphatic amines however afforded both the oxo-urethane and the hydroxyoxazolidone products, the steric hindrance of these amines was assumed to be responsible for slowing down the cyclization step. This step was however accelerated by the addition of DBU as catalyst.

Various poly(hydroxyoxazolidone)s were then synthesized by polyaddition of bisαCCs with the diamines. In line with model reactions, the more sterically hindered cycloaliphatic diamines yielded polymers containing both oxo-urethane and hydroxyoxazolidone linkages. The addition of DBU favored the formation of polymers of higher molar masses. Aliphatic and benzylic diamines provided exclusively poly(hydroxyoxazolidone)s. Some of the polymers, mainly those produced from a bisαCC bearing a cyclohexyl group between the two cyclic carbonate moieties were precipitating during the polymerization and were insoluble in many organic solvents.

We also succeeded in quantitatively dehydrating the different poly(hydroxyoxazolidone)s by refluxing in glacial acetic acid, yielding poly(alkylidene oxazolidone)s. Importantly, two types of oxazolidone linkages with exocyclic olefin moieties were observed depending on the steric hindrance of the poly(hydroxyoxazolidone). For sterically hindered ones, α-alkylidene oxazolidone linkages were selectively formed while a mixture of α- and β-alkylidene oxazolidone linkages (almost in equimolar amounts) were noted for the less bulky ones.

Although the T_g of the poly(hydroxyoxazolidone)s could not be measured due to low polymer degradation temperature, the unsaturated poly(oxazolidone)s presented a high thermal degradation temperature (T_d > 370 °C) with a high T_g (90-130 °C). This novel family of polymers is highly appealing for applications requiring high temperatures. Future works in our laboratory are to exploit the olefins to modify the polymers and to enlarge the scope of this unexplored polymer family. As the reactivity of the two alkylidene oxazolidone linkages are expected to be different, selective modifications should be feasible which should give access to novel functional poly(oxazolidone)s.

AUTHOR INFORMATION

Corresponding Author

*** Christophe Detrembleur:** christophe.detrembleur@uliege.be

Notes

The authors declare no competing financial interest.

ACKNOWLEDGMENT

C.D. thanks the "Fonds National pour la Recherche Scientifique" (F.R.S.-FNRS) and the Fonds Wetenschappelijk Onderzoek – Vlaanderen (FWO) for financial support in the frame of the EOS project n°O019618F (ID EOS: 30902231). The authors from Liege thank the CESAM Research Unit for financial support and the FNRS (Belgium) for funding the research project « CO2Switch » (ID:35289534). C.D. is F.R.S.-FNRS Research Director.

REFERENCES

(1) PlasticsEurope. The Facts 2019. *PlasticsEurope*. 2019.

(2) PlasticsInsight. Polyurethane Production, Pricing and Market Demand.

(3) Wegener, G.; Brandt, M.; Duda, L.; Hofmann, J.; Klesczewski, B.; Koch, D.; Kumpf, R.-J.; Orzesek, H.; Pirkl, H.-G.; Six, C.; Steinlein, C.; Weisbeck, M. Trends in Industrial Catalysis in the Polyurethane Industry. *Appl. Catal. A Gen.* **2001**, *221* (1), 303–335. https://doi.org/https://doi.org/10.1016/S0926-860X(01)00910-3.

(4) Delebecq, E.; Pascault, J.-P.; Boutevin, B.; Ganachaud, F. On the Versatility of Urethane/Urea Bonds: Reversibility, Blocked Isocyanate, and Non-Isocyanate Polyurethane. *Chem. Rev.* **2013**, *113* (1), 80–118. https://doi.org/10.1021/cr300195n.

(5) Engels, H.-W.; Pirkl, H.-G.; Albers, R.; Albach, R. W.; Krause, J.; Hoffmann, A.; Casselmann, H.; Dormish, J. Polyurethanes: Versatile Materials and Sustainable Problem Solvers for Today's Challenges. *Angew. Chemie Int. Ed.* **2013**, *52* (36), 9422–9441. https://doi.org/10.1002/anie.201302766.

(6) Hepburn, C. *Polyurethane Elastomers*; Springer Netherlands, 2012.

(7) Qi, H. J.; Boyce, M. C. Stress-Strain Behavior of Thermoplastic Polyurethanes. *Mech. Mater.* **2005**, *37* (8), 817–839. https://doi.org/https://doi.org/10.1016/j.mechmat.2004.08.001.

(8) Guo, A.; Javni, I.; Petrovic, Z. Rigid Polyurethane Foams Based on Soybean Oil. *J. Appl. Polym. Sci.* **2000**, *77* (2), 467–473. https://doi.org/10.1002/(SICI)1097-4628(20000711)77:2<467::AID-APP25>3.0.CO;2-F.

(9) Cinelli, P.; Anguillesi, I.; Lazzeri, A. Green Synthesis of Flexible Polyurethane Foams from Liquefied Lignin. *Eur. Polym. J.* **2013**, *49* (6), 1174–1184. https://doi.org/https://doi.org/10.1016/j.eurpolymj.2013.04.005.

(10) Panchireddy, S.; Grignard, B.; Thomassin, J.-M.; Jerome, C.; Detrembleur, C. Catechol Containing Polyhydroxyurethanes as High-Performance Coatings and Adhesives. *ACS Sustain. Chem. Eng.* **2018**, *6* (11), 14936–14944. https://doi.org/10.1021/acssuschemeng.8b03429.

(11) Desai, S. D.; Patel, J. V; Sinha, V. K. Polyurethane Adhesive System from Biomaterial-Based Polyol for Bonding Wood. *Int. J. Adhes. Adhes.* **2003**, *23* (5), 393–399. https://doi.org/https://doi.org/10.1016/S0143-7496(03)00070-8.

(12) Deka, H.; Karak, N. Bio-Based Hyperbranched Polyurethanes for Surface Coating Applications. *Prog. Org. Coatings* **2009**, *66* (3), 192–198. https://doi.org/https://doi.org/10.1016/j.porgcoat.2009.07.005.

(13) Jena, K. K.; Raju, K. V. S. N. Synthesis and Characterization of Hyperbranched Polyurethane-Urea/Silica Based Hybrid Coatings. *Ind. Eng. Chem. Res.* **2007**, *46* (20), 6408–6416. https://doi.org/10.1021/ie0703181.

(14) Pankratov, V. A.; Frenkel', T. M.; Fainleib, A. M. 2-Oxazolidinones. *Russ. Chem. Rev.* **1983**, *52* (6), 576–593. https://doi.org/10.1070/rc1983v052n06abeh002864.

(15) Sandler, S. R. Poly-2-Oxazolidones as Cryogenic Adhesives. *J. Appl. Polym. Sci.* **1969**, *13* (12), 2699–2703. https://doi.org/10.1002/app.1969.070131217.

(16) Kinjo, N.; Numata, S.-I.; Koyama, T.; Narahara, T. Synthesis and Viscoelastic Properties of New Thermosetting Resins Having Isocyanurate and Oxazolidone Rings in Their Molecular Structures. *J. Appl. Polym. Sci.* **1983**, *28* (5), 1729–1741. https://doi.org/10.1002/app.1983.070280516.

(17) Sendijarevic, V.; Sendijarevic, A.; Lekovic, H.; Lekovic, H.; Frisch, K. C. Polyoxazolidones for High Temperature Applications. *J. Elastomers Plast.* **1996**, *28* (1), 63–83. https://doi.org/10.1177/009524439602800104.

(18) Kitayama, M.; Isda, Y.; Odaka, F.; Anzai, S.; Irako, K. Synthesis and Properties of Polyoxazolidone Elastomers from Diepoxides and Diisocyanates. *Rubber Chem. Technol.* **1980**, *53* (1), 1–13. https://doi.org/10.5254/1.3535029.

(19) Sendijarevic, V.; Sendijarevic, A.; Frisch, K. C.; Reulen, P. Novel Isocyanate-Based Matrix Resins for High Temperature Composite Applications. *Polym. Compos.* **1996**, *17* (2), 180–186. https://doi.org/10.1002/pc.10603.

(20) Pelzer, T.; Eling, B.; Thomas, H.-J.; Luinstra, G. A. Toward Polymers with Oxazolidin-2-One Building Blocks through Tetra-n-Butyl-Ammonium Halides (Cl, Br, I) Catalyzed Coupling of Epoxides with Isocyanates. *Eur. Polym. J.* **2018**, *107*, 1–8. https://doi.org/https://doi.org/10.1016/j.eurpolymj.2018.07.039.

(21) Speranza, G. P.; Peppel, W. J. Preparation of Substituted 2-Oxazolidones from 1,2-Epoxides and Isocyanates. *J. Org. Chem.* **1958**, *23* (12), 1922–1924. https://doi.org/10.1021/jo01106a027.

(22) Prokofyeva, A.; Laurenzen, H.; Dijkstra, D. J.; Frick, E.; Schmidt, A. M.; Guertler, C.; Koopmans, C.; Wolf, A. Poly-2-Oxazolidones with Tailored Physical Properties Synthesized by Catalyzed Polyaddition of 2,4-Toluene Diisocyanate and Different Bisphenol-Based Diepoxides. *Polym. Int.* **2017**, *66* (3), 399–404. https://doi.org/10.1002/pi.5279.

(23) Herweh, J. E.; Whitmore, W. Y. Poly-2-Oxazolidones: Preparation and Characterization. *J. Polym. Sci. Part A-1 Polym. Chem.* **1970**, *8* (10), 2759–2773. https://doi.org/10.1002/pol.1970.150081004.

(24) Altmann, H. J.; Clauss, M.; König, S.; Frick-Delaittre, E.; Koopmans, C.; Wolf, A.; Guertler, C.; Naumann, S.; Buchmeiser, M. R. Synthesis of Linear Poly(Oxazolidin-2-One)s by Cooperative Catalysis Based on N-Heterocyclic Carbenes and Simple Lewis Acids. *Macromolecules* **2019**, *52* (2), 487–494. https://doi.org/10.1021/acs.macromol.8b02403.

(25) Iwakura, Y.; Izawa, S.-I.; Hayano, F. Polyoxazolidones Prepared from Bisurethans and Bisepoxides. *J. Polym. Sci. Part A-1 Polym. Chem.* **1966**, *4* (4), 751–760. https://doi.org/10.1002/pol.1966.150040402.

(26) Yoo, W.-J.; Li, C.-J. Copper-Catalyzed Four-Component Coupling between Aldehydes, Amines, Alkynes, and Carbon Dioxide. *Adv. Synth. Catal.* **2008**, *350* (10), 1503–1506. https://doi.org/10.1002/adsc.200800232.

(27) Teffahi, D.; Li, S. H.; Chao-Jun. Synthesis of Oxazolidinones, Dioxazolidinone and Polyoxazolidinone (A New Polyurethane) Via A Multi Component-Coupling of Aldehyde, Diamine Dihydrochloride, Terminal Alkyne and CO2. *Letters in Organic Chemistry*. 2012, pp 585–593. https://doi.org/http://dx.doi.org/10.2174/157017812802850221.

(28) Wu, Q.; Chen, J.; Guo, X.; Xu, Y. Copper(I)-Catalyzed Four-Component Coupling Using Renewable Building Blocks of CO2 and Biomass-Based Aldehydes. *European J. Org. Chem.* **2018**, *2018* (24), 3105–3113. https://doi.org/10.1002/ejoc.201800461.

(29) Gennen, S.; Grignard, B.; Tassaing, T.; Jérôme, C.; Detrembleur, C. CO2-Sourced α-Alkylidene Cyclic Carbonates: A Step Forward in the Quest for Functional Regioregular Poly(Urethane)s and Poly(Carbonate)S. *Angew. Chemie Int. Ed.* **2017**, *56* (35), 10394–10398. https://doi.org/10.1002/anie.201704467.

(30) Grignard, B.; Gennen, S.; Jérôme, C.; Kleij, A. W.; Detrembleur, C. Advances in the Use of CO2 as a Renewable Feedstock for the Synthesis of Polymers. *Chem. Soc. Rev.* **2019**, *48* (16), 4466–4514. https://doi.org/10.1039/C9CS00047J.

(31) Ouhib, F.; Grignard, B.; Van Den Broeck, E.; Luxen, A.; Robeyns, K.; Van Speybroeck, V.; Jerome, C.; Detrembleur, C. A Switchable Domino Process for the Construction of Novel CO2-Sourced Sulfur-Containing Building Blocks and Polymers. *Angew. Chemie Int. Ed.* **2019**, *58* (34), 11768–11773. https://doi.org/10.1002/anie.201905969.

(32) Delidovich, I.; Hausoul, P. J. C.; Deng, L.; Pfützenreuter, R.; Rose, M.; Palkovits, R. Alternative Monomers Based on Lignocellulose and Their Use for Polymer Production. *Chem. Rev.* **2016**, *116* (3), 1540–1599. https://doi.org/10.1021/acs.chemrev.5b00354.

(33) Upton, B. M.; Kasko, A. M. Strategies for the Conversion of Lignin to High-Value Polymeric Materials: Review and Perspective. *Chem. Rev.* **2016**, *116* (4), 2275–2306. https://doi.org/10.1021/acs.chemrev.5b00345.

(34) Francis, T.; Thorne, M. P. Carbamates and 2-Oxazolidinones from Tertiary Alcohols and Isocyanates. *Can. J. Chem.* **1976**, *54* (1), 24–30. https://doi.org/10.1139/v76-006.

(35) Hase, S.; Kayaki, Y.; Ikariya, T. Mechanistic Aspects of the Carboxylative Cyclization of Propargylamines and Carbon Dioxide Catalyzed by Gold(I) Complexes Bearing an N-Heterocyclic Carbene Ligand. *ACS Catal.* **2015**, *5* (9), 5135–5140. https://doi.org/10.1021/acscatal.5b01335.